Novel high-breakdown InGaAs/InAlAs pHEMTs for radio astronomy applications

A.Bouloukou[(1)], A. Sobih[(1)], D. Kettle[(2)], J. Sly[(1)] and M. Missous[(1)]

[(1)]School of Electrical and Electronic Engineering
Email: a.bouloukou@postgrad.manchester.ac.uk

[(2)]School of Physics and Astronomy
University of Manchester, Manchester M60 1QD

Abstract
By optimising the epitaxial layer profile of InGaAs-InAlAs pHEMTs we have demonstrated improved DC and RF performance from a new, low-cost, 1 µm-gate device structure in terms of breakdown voltage, leakage current and output conductance. A simple fabrication process is employed that does not use double-recess or composite-channel structures. No penalty was incurred on cut-off frequency or gain due to this new design approach. High uniformity of device characteristics across wafers and between different process runs has been achieved by utilising highly optimised and controlled processing techniques. The room-temperature noise characteristics of these devices are better than 0.5 dB at 1.4 GHz and they show great potential for low-cost, ultra-low-noise LNAs operating at room temperature in the low-frequency radio astronomy band.

Keywords: InP pHEMT, breakdown voltage, radio astronomy, MBE, low noise

1. INTRODUCTION

In the last decade considerable progress has been made in the design and fabrication of ultra-low-noise receivers and amplifiers using InP-based pseudomorphic High Electron Mobility Transistors (pHEMTs). However, conventional low-noise InGaAs-InAlAs pHEMTs currently used in both low-noise amplifier (LNA) and power amplifier (PA) designs suffer from poor linearity and inherently low breakdown voltages (V_{BDG}) almost regardless of gate length [1]: typically $V_{BDG} \approx$ 2-4 V. This compromises and complicates LNA designs for rugged, room-temperature radio astronomy (RA) applications. The poor breakdown voltages have generally been attributed to impact ionisation in the low bandgap channel material. Attempts at increasing the off-state breakdown voltage have been reported over the years. These have usually comprised materials modifications to the basic pHEMT design, such as (a) the use of InAlAs buffers grown at low temperature [2], (b) the use of AlAs, InAlP or InGaP supply layers for enhanced Schottky barriers (and consequent large hole barriers to reduce hole injection from the channel) [3-5], and (c) the use of composite-channel designs [6] or purely geometrical modifications, such as double-recessed structures [7], for electric field manipulation. While successful in raising V_{BDG} to 6-10 V, most of these approaches are compromised by a severe drop in the unity current gain cut-off frequency, F_T (and hence an increase in noise), and a drop in current-driving capability. Furthermore, the low Schottky barrier formed by common gate metals on InGaAs usually leads to a side-gate-leakage current with a consequent low breakdown voltage [8]. So, it is clear that the problem of the reduced V_{BDG} is far from being solved.

For the upcoming Square Kilometre Array (SKA) telescope [9], rugged (i.e. high breakdown), high-performance (i.e. low noise and high gain), room-temperature operation is paramount. There is also a requirement for low cost because, in the aperture array concept of the SKA, hundreds of millions of amplifiers would be needed and while existing commercial devices (mainly 0.1 µm-gate, InP–based pHEMTs) are able to fulfil some of the requirements of SKA, their cost and breakdown fragility precludes their use in this particular application. Our devices achieve improved RF performance predominantly through bandgap engineering rather than scaling. This 'materials' approach enhances V_{BDG} without the use of double-recesses or side-gate-leakage reduction steps and, from a manufacturability viewpoint, the 'relaxed' optical lithography will be more cost effective than nanoscale lithography in either Si or InP technology.

Here, we present the results of on-going work to develop room-temperature-operated devices for use in the low-frequency band of the SKA (200 MHz to 2 GHz). We have designed, fabricated and characterised a family of InP-based pHEMTs with 1 µm gate geometries. The results of DC and microwave measurements demonstrate that these devices give state-of-the-art RF performance, compared to the best 1 µm devices reported in the literature, and have a V_{BDG} in excess of 14 V.

2. EXPERIMENTAL

The structures under investigation were grown in-house using solid-source Molecular Beam Epitaxy (MBE) on an Oxford Instruments V90H system. They are based on an InGaAs/InAlAs/InP epitaxial layer design and consist of an

InAlAs buffer, strained $In_{0.7}Ga_{0.3}As$ channel, δ-doped InAlAs supply layer and undoped InGaAs cap layer. A generic structure and its associated band diagram (calculated using WinGreen [10]) are shown in Fig. 1.

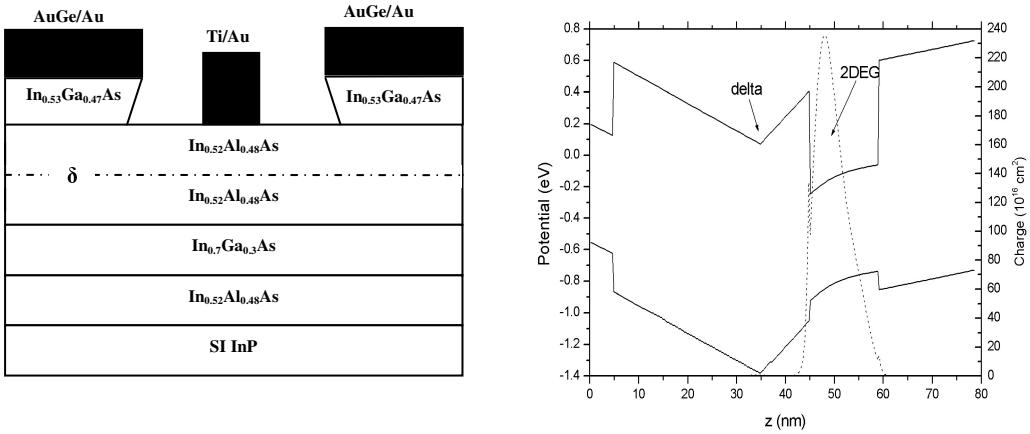

Fig. 1. Generic pHEMT structure and associated band diagram

The epitaxial structure consists of a single heterostructure, with a carefully designed supply layer so that the 2-dimensional electron gas (2DEG) population is optimised. Two different structures were studied; a conventional pHEMT (VMBE1855), grown under standard conditions [1] and an 'improved' structure (VMBE1831). The main difference in the two structures is the way in which the 2DEG is populated from the supply layer. This was determined by careful control of the spacer layer and the supply-layer doping (detailed growth parameters are given elsewhere [11]). Both structures have undoped cap layers to allow non-destructive on-wafer IV and CV measurements to be made prior to device fabrication.

Devices with a nominal 1μm gate length were fabricated concurrently, to minimise processing inconsistencies, using standard optical lithography. Mesas were defined by wet-etching, down to the InAlAs buffer layer, using a non-selective etch (H_3PO_4:H_2O_2:H_2O in the ratio 3:1:50). For the ohmic contacts, 50 nm of AuGe followed by 220 nm of Au was thermally evaporated and alloyed at 260°C, yielding a contact resistance of 0.2 Ω.mm. A highly selective adipic acid etch [12] was then used to remove the InGaAs cap layer, forming a wide gate recess as shown in Fig. 1. Ti (50 nm) and then Au (100 nm) were thermally evaporated to form the gate contact. Finally, bond/probe pads were deposited (50 nm of Ti and 450 nm of Au) and sintered (at 250°C) to enable microwave probing for on-wafer RF measurements.

3. RESULTS AND DISCUSSION

3.1. DC Characteristics

Material quality was assessed by Hall effect measurements. The as-grown sheet carrier density, N_s, and mobility, μ, for the improved (VMBE1831) and conventional (VMBE1855) pHEMTs were N_s=1.87x10^{12} cm^{-2}, μ=13244 cm^2/V.s and N_s=2.43x10^{12} cm^{-2}, μ=12627 cm^2/V.s respectively, indicating not only excellent material quality but also similar 2DEG properties. Virtually no freeze-out was observed at 77 K and mobilities in both cases were greater than 56,000 cm^2/V.s. The on-wafer IV and CV characteristics of both structures are shown in Fig. 2.

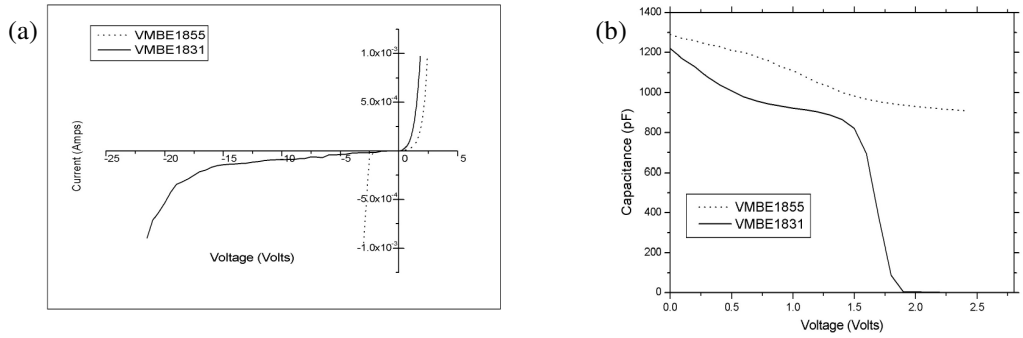

Fig. 2. (a) IV and (b) CV characteristics of VMBE1855 and 1831 obtained on-wafer by Mercury prober

It is clear from Fig. 2(a) that the new structure (VMBE1831) has a much-improved breakdown voltage (>15 V compared to ~3 V) and leakage currents are in the low µA-range, despite the very large Schottky contact areas used on-wafer (~500,000 μm^2, which is ~1000 times higher than pHEMT gate areas). A clear pinch-off voltage is observed for the new structure but not for the conventional one because of the low breakdown voltage. These results are replicated in the fabricated transistors (Fig. 3), with V_{BDG} >14 V.

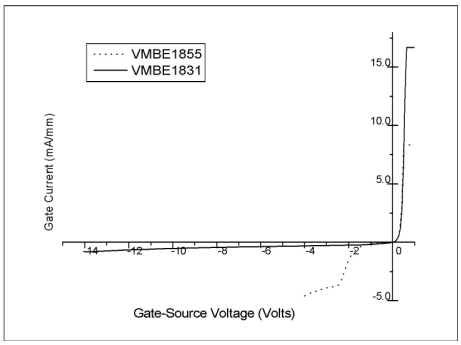

Fig. 3: Comparison of gate-drain diode IV characteristics (1x200 µm device)

The pHEMT characteristics of VMBE1831 are shown in Fig. 4(a). These show extremely well-behaved curves with a sharply defined pinch-off, a small output conductance and a very small amount of kink effect (indicating little carrier loss under low gate-bias). The corresponding data for the conventional pHEMT is shown in Fig. 4(b) where the effect of the leakage is translated into a larger output conductance.

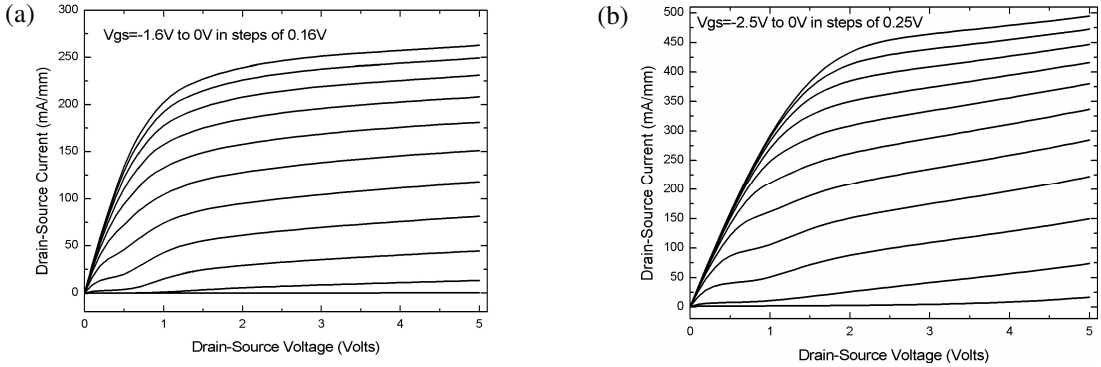

Fig. 4. Common source output characteristics for (a) VMBE1831 and (b) VMBE1855 (1x60 µm devices)

3.2. RF Characteristics

The RF parameters were extracted from on-wafer probe measurements performed using an HP8510C vector network analyser in the range 45 MHz to 40 GHz. The current–gain frequency curves for both devices are shown in Fig. 5.

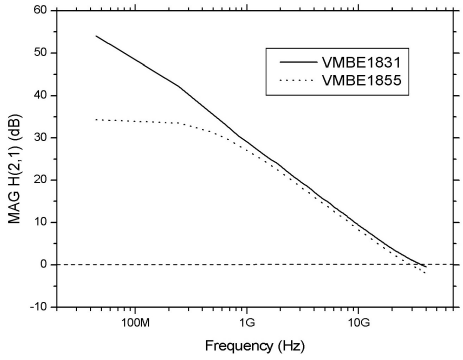

Fig. 5. Current gain of a 1x120 µm (#1831) and 1x100 µm (#1855) transistor

The measured unity current gain cut-off frequencies are 37 GHz and 30 GHz for the new and conventional devices respectively. These represent excellent values for the gate geometry used here.

The linear small-signal model parameters were extracted from the measured S-parameter analytically, using standard computer-aided design (CAD) tools [13-15]. The 7 intrinsic model parameters were obtained from hot (active) device bias points, while the 8 extrinsic (parasitic) elements were obtained from cold (pinched) device measurements [16-19]. The equivalent circuit of the linear model is shown in Fig. 6. The final element values for this model, shown in table 1, were determined by applying CAD optimization techniques to the initial values obtained, until the model accurately fitted the measured data.

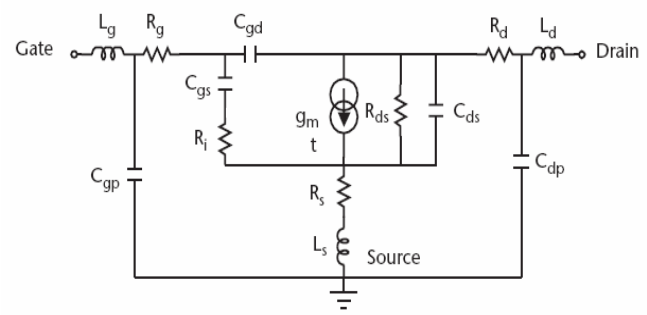

Fig. 6. Small-signal equivalent circuit model of the fabricated pHEMT [16]

Table 1. Extracted element values of the device models

Device_Sample#1831 (Lg=1µm , Wg= 120 µm)				Device_Sample#1855 (Lg=1µm , Wg= 100 µm)			
Element	Value	Element	Value	Element	Value	Element	Value
Gm(mS)	38	Rs(Ω)	3.33	Gm(mS)	43	Rs(Ω)	2.88
T(ps.)	1.41	Rg(Ω)	13.43	T(ps.)	0.64	Rg(Ω)	17.92
Ri(Ω)	9.1	Rd(Ω)	3.93	Ri(Ω)	11.4	Rd(Ω)	9.26
Gds(mS)	1.42	Ls(pH)	4.45	Gds(mS)	1.89	Ls(pH)	2.34
Cgs(pF)	0.176	Lg(pH)	12.96	Cgs(pF)	0.207	Lg(pH)	29.23
Cds(pF)	0.0337	Ld(pH)	35.74	Cds(pF)	0.0359	Ld(pH)	21.17
Cgd(pF)	0.0174	Cpg(fF)	1.29	Cgd(pF)	0.0163	Cpg(fF)	14.82
		Cpd(fF)	27.1			Cpd(fF)	27.24

Fig. 7 shows a comparison between the measured and modelled S-parameters of the pHEMT devices, illustrating the excellent agreement between the measured data and the equivalent circuit models. The large values of the channel resistance, R_i, are attributed to biasing these devices near the pinch-off voltage.

(a)

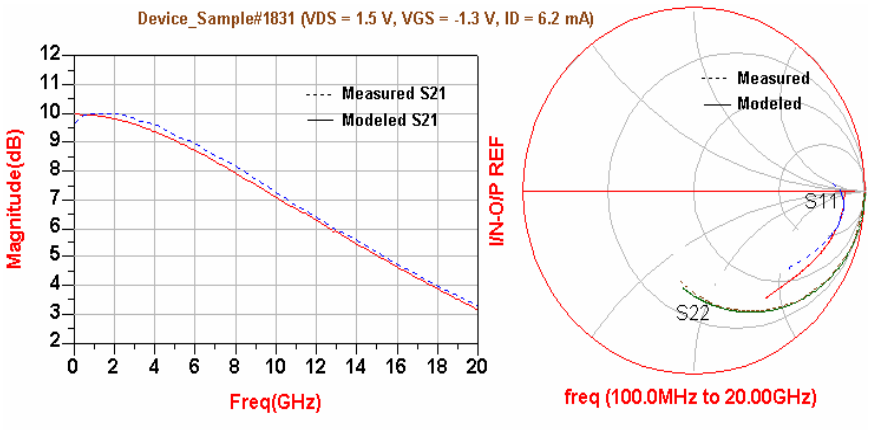

(b)

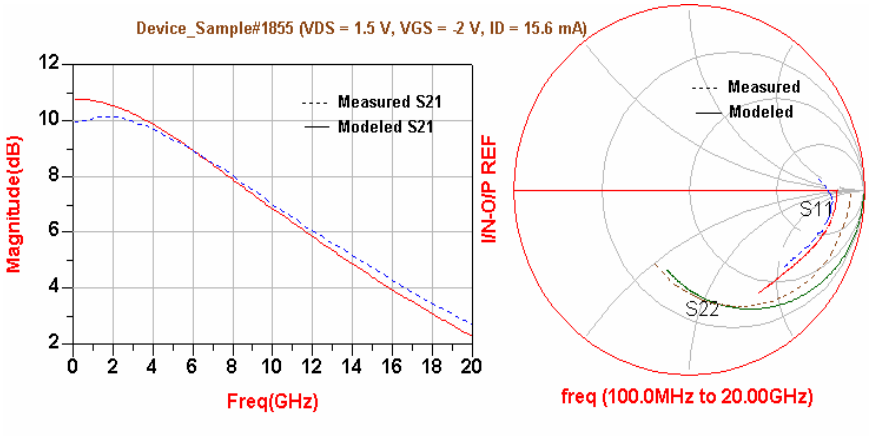

Fig. 7. Comparison between modelled and measured S-parameters of (a) VMBE1831 and (b) VMBE1855

Predicted, room-temperature, minimum noise figures are shown in Fig. 8, up to 20 GHz, for the two structures. It is clear that the noise characteristics are better for the improved device, reflecting the effect of the reduced leakage current. This effect is more pronounced at higher frequencies. At 1.4 GHz the noise figure is less than 0.5 dB (35 K noise temperature, Fig. 8 insert), in these geometrically unoptimised (in terms of gate resistance and gate width) devices.

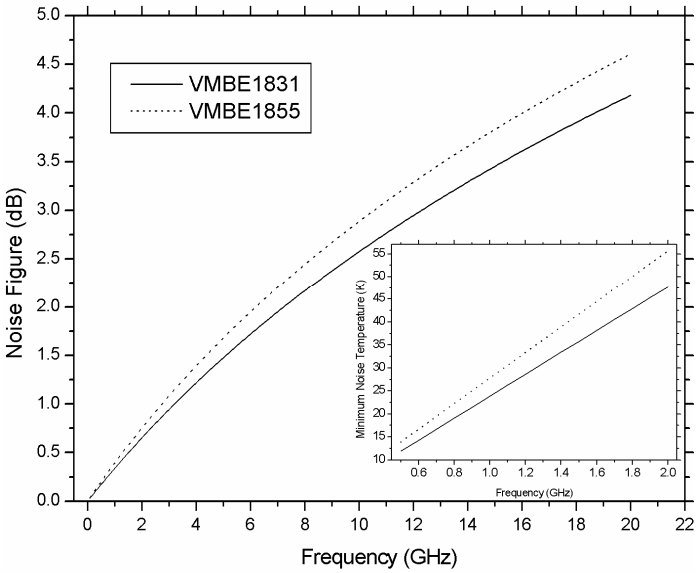

Fig. 8. Comparison of minimum noise figures of the improved (VMBE1831) and conventional (VMBE1855) pHEMTs

4. CONCLUSIONS

In conclusion, we have demonstrated improved DC and RF characteristics from a new design of InGaAs-InAlAs pHEMT. Significant improvements have been made to the breakdown voltage, leakage current and output conductance by means of careful epilayer design in conjunction with a simple, but highly optimised and controlled, fabrication process. Complex double-recess and composite-channel techniques have been avoided and high uniformity and reproducibility has been achieved. Microwave measurements indicate that no penalty has been incurred in terms of cut-off frequency or gain. The predicted noise figures of these devices are better than those of conventional low-breakdown, 1 µm-gate devices. These devices, therefore, have great potential for low-cost, ultra-low-noise LNAs for radio astronomy applications such as aperture and focal-plane arrays operating in the 200 MHz to 2 GHz band.

5. ACKNOWLEDGEMENTS

This work was suported by The UK's Particle Physics and Astronomy Research Council (PPARC) under the 'Innovative Technology Fund' programme.

6. REFERENCES

[1] U.K Mishra, A.S. Brown, L.M. Jelloian, L.H Hackett and M.J. Delaney, "High-performance sub micrometer AlInAs-GaInAs HEMT's", *Electron Device Letters,* 9(1), pp. 41, 1988.

[2] W. Prost and F.J. Tegude, "High speed, high gain InP-based heterostructure FETs with high breakdown voltage and low leakage", *Proc. 8th IPRM*, pp. 729, 1996.

[3] U. Auer, R. Reuter, P. Ellrodt, C. Heedt, W. Prost and F. J. Tegude, "The impact of pseudomorphic AlAs spacer layers on the gate leakage current of InA1As /InGaAs heterostructure field-effect transistors", *Proc. 8th IPRM*, pp. 424, 1996.

[4] Yasuro Yamane, Haruki Yokoyama, Takashi Makimura, Takashi Kobayashi and Yasunobu Ishii, "0. l-µm InAlP/InAlAs/InGaAs/InP HEMTs with improved breakdown voltages", *Proc. 11th IPRM*, pp. 311, 1999.

[5] F. Scheffer, C. Heedt, R. Reuter, A. Lindner, Q. Liu, W. Prost and F. J. Tegude, "High breakdown voltage InGaAs/lnAIAs HFET using InGaP spacer layer", *Electronics Letters,* vol. 30(2), pp.169, 1994.

[6] N. Cavassilas, F. Aniel, P. Boucaud, R. Adde, H. Maher, J. De´ cobert and A. Scavennec, "Electroluminescence of composite channel InAlAs-InGaAs-InP-InAlAs high electron mobility transistor", *J.Appl.Phys.,* vol. 87(5), pp. 2548, 2000.

[7] K.Y. Hur, R.A. McTaggart, P.J. Lemonias, andW.E. Hoke, "Development of double recessed AlInAs/GaInAs HEMTs for millimetre wave power applications", *Solid State Electronics,* vol. 41(10), pp. 1581, 1997.

[8] S.R**.** Bahl**,** M. H. Leary and J.A. del Alamo, "Mesa-Sidewall Gate Leakage in InAlAs/InGaAs Heterostructure Field-Effect Transistors*", IEEE Trans. Electron. Dev., vol.* 39(9), pp. 2037, 1992.

[9] SKA – *Square Kilometre Array*, http://www.skatelescope.org, viewed 14th November 2005.

[10] K. M. Indlekofer and J. Malindretos, *WinGreen Simulation Package*, http://www.fz-juelich.de/isg/mbe/software.html (Research Centre J¨ulich), viewed 21st December 2005.

[11] M. Missous, *patent pending*

[12] K. Higuchi, H. Uchiyama, T. Shiota, M. Kudo and T. Mishima, "Selective wet-etching of InGaAs on InAlAs using adipic acid and its application to InAlAs/InGaAs HEMTs", *Semicond. Sci. Technol.*, vol. 12, pp. 475-480, 1997.

[13] N. Rorsman, M. Garcia, C. Karlson and H. Zirath, "Accurate Small-signal Modeling of HFETs for Millimeter-wave Applications", *IEEE Trans. Microwave Theory Tech*, vol. 44(3), pp. 432-437, March 1996.

[14] F. E. Patiño and J. R. Pérez, "Modeling and simulation of pseudomorphic HEMT's for analog circuit design and analysis", *ELECTRO 2001*, pp. 277-282, 2001.

[15] M. Berroth and R. Bosch, "Broad-Band Determination of the FET Small-Signal Equivalent Circuit", *IEEE Trans. on Microwave Theory and Techniques*, vol. 38(7), pp. 891–895, July 1990.

[16] B. S. Virdee, A. S. Virdee and B. Y. Banyamin, *Broadband Microwave Amplifiers*, Chapter-4, pp. 83, Boston: Artech House Inc., 2004.

[17] R. Anholt and S. Swirhun, "Equivalent-circuit parameter extraction for cold GaAs MESFET's," *IEEE Trans. Microwave Theory Tech.*, vol. 39, pp. 1243-1247, July 1991.

[18] E. Arnold, M. Golio, M. Miller and B. Beckwith, "Direct extraction of GaAs MESFET intrinsic element and parasitic inductance values", *IEEE MTT-S International Microwave Symposium Digest*, vol. 1, pp. 359-362, 1990.

[19] Paul M. White and Richard M. Healy, "Improved Equivalent Circuit for Determination of MESFET and HEMT Parasitic Capacitances from "Coldfet" Measurements" *IEEE Microwave and Guided Wave Letters*, vol. 3(12), December 1993.